7th Power Electronics, Drive Systems & Technologies Conference (PEDSTC 2016)
16-18 Feb. 2016, Iran University of Science and Technology, Tehran, Iran

An Interleaved High-Power Two-Switch Flyback Inverter with a Fast and Robust Maximum Power Point Tracker

Saleh Mohammadi
Dept. of Electrical Engineering
Bojnord Branch, Islamic Azad University
Bojnord, Iran
Saleh.67mohammadi@yahoo.com

H.Abootorabi Zarchi
Dept. of Electrical Engineering
Ferdowsi University of Mashhad
Mashhad, Iran
abootorabi@um.ac.ir

***Abstract*— The major drawback of the two switch flyback topology is its low-power applications such as microinverter. This study proposes a high-power two-switch flyback inverter and shows its excellent performance as a string-type PV inverter. The suggested inverter system is based on interleaving technique and operated in discontinuous conduction mode. Moreover, a fast and robust maximum power point tracking method is proposed. The fast dynamics and robustness of the proposed method is achieved using variable structure control approach. Simulation results with a 2 kW inverter system confirm the excellent performance of the suggested scheme. The total harmonic distortion and power factor are measured as 2% and 0.99 respectively. Therefore, it is shown that the performance of the suggested system is comparable to the common isolated PV inverters available in the market.**

Keywords—two switch flyback; variable structure control; THD; power factor; MPPT.

I. INTRODUCTION

Nowadays, environmental concerns and freely available nature of photovoltaic (PV) energy have caused extensive applications of this important source of energy [1]. In photovoltaic systems, the flyback converter is considered as an appropriate topology due to advantages of fewer component count, simplicity and isolation between the PV modules and grid line [2]. One of the biggest drawbacks of the flyback inverter is the high voltage and current stresses of the switches which suffers them. A switch with higher voltage rating is required to withstand the turn-off transient voltage. Consequently the size and cost of the switch is increased. Moreover the on-resistance of the switch is increased, resulting in increased conduction losses [3].

The two switch flyback converter is an appropriate solution to reduce the voltage stress of the switches. The switch voltage stress in this converter is decreased to the dc input voltage, reducing the switching and conduction losses. The additional switch and the main one operate homogeneously, therefore the control logic is very simple [4], [5].

The design of a transformer with large energy storage capability is always a challenge. The air gap where the energy is stored is very large in high-power flyback converter. As a result of this, the leakage flux is increased and efficiency of the converter is decreased. Chiefly this reason most often causes that the flyback converters are designed for low power applications. However, if we apply modern and optimal designing schemes properly, this converter topology can be applied in high-power too. Interleaving of flyback inverters assists designing high-power flyback inverters. Furthermore, when the number of interleaved cells increased, the frequency of harmonics at the waveform are increased as well. This feature makes it easy to filter out the harmonics by using smaller sized filtering elements. Therefore the cost of passive elements are reduced [6], [7].

In contrast to pulse width modulated (PWM) based maximum power point tracking (MPPT), we propose a sliding mode controlled MPPT. Variable structure or sliding mode controlled MPPT presents a fast response to variations in radiation. In addition, the implementation of the control is simple and requires low cost hardware. This work may be viewed as an extension of the work by Levron and Shmilovitz [8]. The authors proposed an MPPT controller based on an inner sliding-mode loop which uses inductor's current as the main state variable. This method is generally more robust and stable, but the switching frequency cannot be determined exactly. Also, the maximum power point (MPP) voltage affects the switching frequency, thus, the switching frequency changes with the temperature and the design of the controller is complicated and may cause instability. A MPPT method is suggested in [9] based on variable structure control approach and P-I characteristic of the PV panel which has a slow response to variation in radiation.

The main goal of this study is to design and suggest a grid-tied, isolated and string-type inverter based on the two-switch flyback converter topology at 2 kW, which is not available in today's PV market. Moreover, a new fast and robust MPPT technique is presented which is based on variable structure control approach. The suggested control system adjusts the switching frequency precisely and independent to MPP voltage. So the switching frequency doesn't change in case of

978-1-5090-0375-4/16/$31.00 ©2016 IEEE

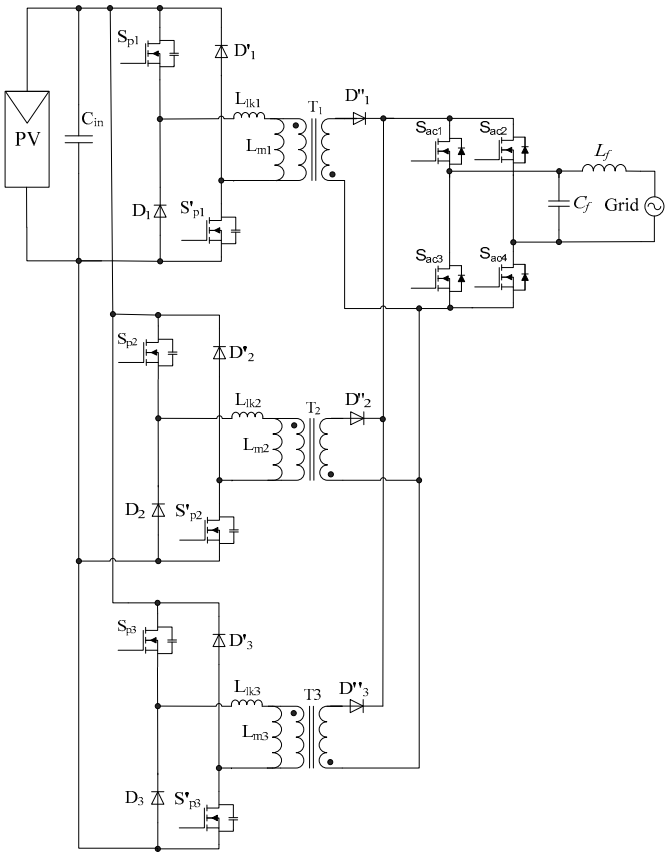

Fig. 1: Schematic diagram of the suggested PV inverter system

variation in temperature. The proposed system has performed effectively according to the main specifications such as the power factor and the THD of the grid current.

This paper has five main parts. Part II introduces the proposed topology. Design steps are stated in part III and design equations are derived. The proper operation of the introduced scheme is confirmed through simulations presented in part IV. The last part provides the conclusions.

II. CONVERTER DESCRIPTION AND ANALYSIS

A. Proposed Structure

Fig. 1 shows the proposed PV inverter system. The proposed system consists of five main parts: first-phase converter, second-phase converter, third-phase converter, unfolding bridge, and C–L filter. S_{Pi}, $S'_{Pi\ (i=1,\ 2,\ 3)}$ are the main power switches; D''_i is the rectifier diode; L_{lki} is the Leakage inductance, and L_{mi} is the magnetizing inductance. Unfolding the rectified sinusoidal waveform for attaching to the grid is done with a current source inverter formed by S_{ac1}-S_{ac4}. D_i and D'_i are clamping diodes.

B. Operational Analysis of the Proposed Structure

Steady-state performance of the system is composed of four operational modes in a switching period. The simplicity of the control encouraged us to apply discontinuous conduction mode (DCM) in design of the proposed scheme. The principle of the operation of each stage is explained according to the equivalent circuits of the first-phase converter shown in Fig. 2 and the voltage and current waveforms of the converter shown in Fig. 3.

Stage 1 ($t_0 < t < t_1$): At the beginning of this stage, switches S_{P1} and S'_{P1} are turned on. The PV panel voltage is across the primary winding. So, the current of magnetizing and leakage inductances increases linearly. The current of L_{m1} and L_{lk1} can be stated as:

$$i_{Lm1} = i_{Llk1} = \frac{V_{pv}}{L_{m1} + L_{lk1}}(t - t_0) + i_{Lm1}(t_0) \tag{1}$$

Where $i_{Lm1}(t_0) = 0$. The equation of the peak current of L_{m1} can be written as follows:

$$i_{Lm1}(t_1) = \frac{V_{pv}\, d\, T_s}{L_{m1} + L_{lk1}} \tag{2}$$

In (2), d and dT_s are the duty cycle and on time of the main switches S_{P1} and S'_{P1} in a particular switching cycle respectively. The peak current of the magnetizing inductance has a sinusoidal waveform. So we have:

$$d(t) = d_{\max} \sin(\omega t) \tag{3}$$

d_{max} refers to maximum duty cycle. At the end of this stage the switches S_{P1} and S'_{P1} are turned off.

Stage2 ($t_1 < t \le t_2$): In this stage, the reflected output voltage $-nV_g$ ($0 \le Vg \le 220\sqrt{2}$) is put across the primary winding and the voltage across the switches S_{P1} and S'_{P1} is limited to V_{pv}. The energy stored in L_{lk1} charges the input capacitance C_{in} through diodes D_1 and D'_1. So, we have:

$$i_{Lm1} = i_{Llk1} = -\frac{V_{pv}}{L_{m1} + L_{lk1}}(t - t_1) - i_{Lm1}(t_1) \tag{4}$$

$i_{Lm1}(t_1)$ refers to the initial current of the magnetizing inductance at $t = t_1$. At the end of this stage, i_{Llk1} drops to zero. Thus, clamping diodes D_1 and D'_1 are turned off.

Stage3 ($t_2 < t \le t_3$): In this stage, all the energy stored in L_{m1} is transferred to the secondary side. An equivalent circuit for this stage is depicted in Fig. 2(c). The voltage of $-nV_g$ is put across the magnetizing inductance. So, the current passes through the magnetizing inductance is equal to:

$$i_{Lm1} = -\frac{nV_g}{L_{m1}}(t - t_2) + i_{Lm1}(t_2) \tag{5}$$

i_{Lm1} (t_2) refers to the initial current of L_{m1} at time t_2. If we consider that the switches S_{P1}, S'_{P1} are identical, the voltages across them is represented as follows:

$$V_{SP1} = V_{S'P1} = \frac{V_{pv} + nV_g}{2} \tag{6}$$

Stage4 $(t_3 < t \le t_4)$**:** In this stage, the energy stored in C_f and L_f is transferred to the grid. The voltage across S_{P1} and S'_{P1} is represented as follows:

$$V_{SP1} = V_{S'P1} = \frac{V_{pv}}{2} \tag{7}$$

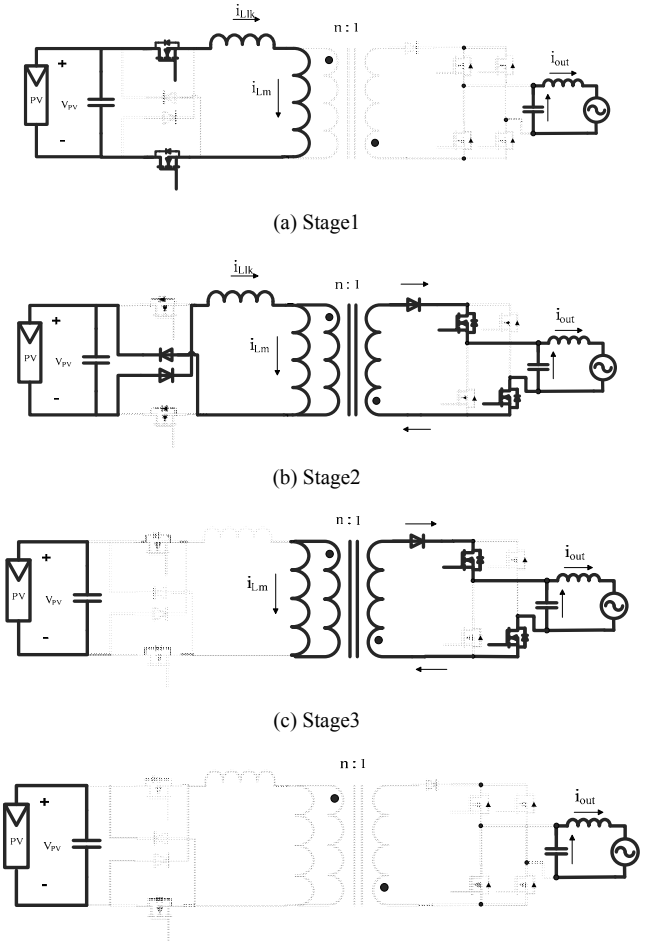

(a) Stage1

(b) Stage2

(c) Stage3

(d) Stage4

Fig.2 Equivalent circuits of the proposed system in steady-state operation

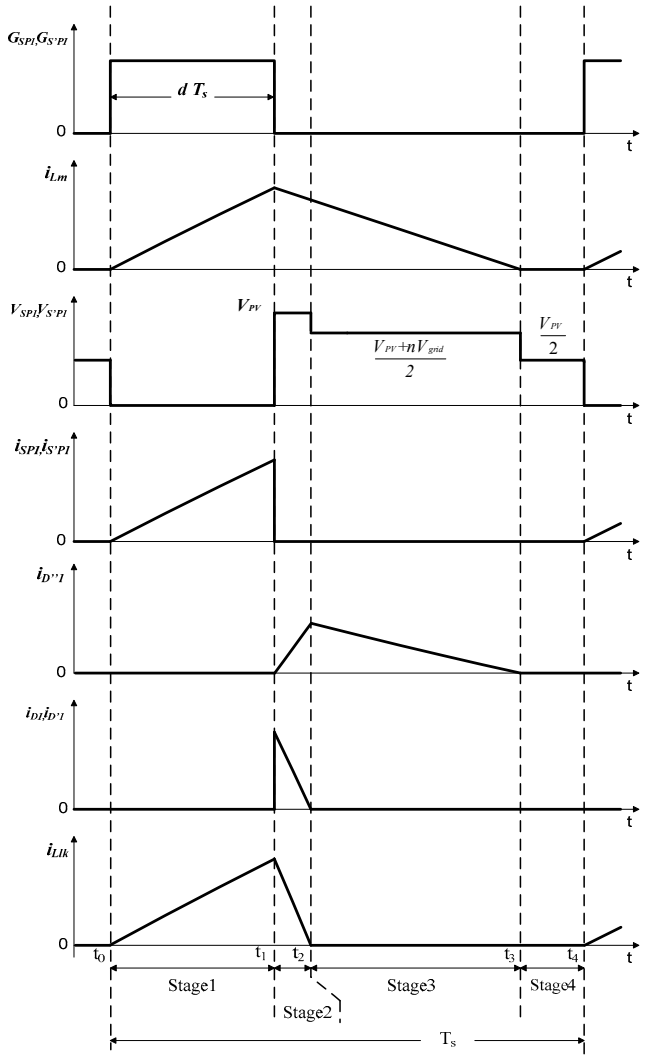

Fig. 3 Voltage and current waveforms of the proposed structure

III. DESIGN PROCEDURE

A. Parameters Design

The main specifications for designing the proposed inverter system is summarized in Table I. When the switches S_{Pi} and S'_{Pi} are turned off, we should prevent conduction of D_i, D'_i and also prevent transferring the energy stored in magnetizing inductance energy to the input capacitor. So, two important limitations in designing the inverter system should be considered as follows:

$$nV_m < V_{pv} \tag{8}$$

$$d_{\max} < 0.5 \tag{9}$$

In (8), V_m refers to the peak value of the output voltage. Two-thirds of V_{pv} is an appropriate peak value of reflected output voltage nV_m [10].

TABLE I. DESIGN SPECIFICATIONS

Design parameters	Specifications
PV model and maximum power	JC250M,250 W
Open circuit voltage and short circuit current per panel	37.4 V,8.83 A
Maximum power current and voltage per panel and per the selected panel group arrangement	30.1 V,8.31 A,240.8 V,8.31 A
Total maximum dc power from the PV array	2000 W
Grid characteristics	Single-phase, 220 V, 50 Hz
Grid current percent THD	<5%
Power factor	>0.99
Switching frequency	20 kHz
Number of interleaved cells	3

Following equation should be considered for determining maximum duty cycle d_{max} [7]:

$$d_{\max} \le (1+\frac{V_{pv}}{nV_m})^{-1} \tag{10}$$

For $V_m = 220\sqrt{2}$ V and V_{pv}=240.8 V, turn ratio should be n < 0.77. We select n=0.33 considering the above limitations.

In [11], the average primary current value is described as follows:

$$I_{P,avg} = \frac{n_{cell} V_{pv} T_s d_{\max}^{\ 2}}{4L_m} \tag{11}$$

The input power of interleaved flyback inverter is:

$$P_{pv} = V_{pv} I_{p,avg} = \frac{n_{cell} V_{pv}^{\ 2} T_s d_{\max}^{\ 2}}{4L_m} \tag{12}$$

For P_{PV}=2000 W, V_{pv}=240.8 V and d_{max}=0.3, the maximum transformer magnetizing inductance is equal to $L_{m,max}$=97.8 μH.

B. Reference Current design

In order to regulate the output current, the reference signal for each phase is obtained as follows[7]:

$$i_{refi} = \sin(\omega t)\sqrt{\frac{4P_o}{n_{cell} L_m f_s}} \tag{13}$$

C. Proposed MPPT control method

The PV generators (PVG) exhibit nonlinear *I–V* and *P–V* characteristic curves. The maximum power produced depends on both irradiance and temperature. Reference [8] with the aid of *I-V* curves of PV panel, defines a switching surface that satisfies MPPT regarding irradiance. The proposed surface in [8] is:

$$S(V, i) = a\, i - b\, V + ref = 0 \tag{14}$$

Where *V* and *i* are PV panel output voltage and current, and *a, b,* and *ref* define the switching surface. Fig. 4, shows the proposed surface. The switching frequency is dependent on MPP voltage and has different value when the temperature changes according to (15) [8].

$$f_{sw} = \frac{aV_{mpp}}{\Delta . L}(1-\frac{V_{mpp}}{V_o}) \tag{15}$$

Moreover, the designed switching frequency has a 20% error in comparison with experimental result. Thus, the design of the controller system can be a complicated one. By comparison, in this work we design the switching frequency precisely and independent on MPP voltage.

The schematic diagram of the system in presence of proposed control scheme is illustrated in Fig. 5. The main part of it is "linear and variable structure control" (LVSC) which comprises the sliding-mode and linear controller. This controller takes advantage of the best specifications of the linear controller like, smooth operation and the best features of variable structure control that are, robustness to perturbations and modeling uncertainties. In the proposed system, the MPPT control system consists of sliding-mode controller with an adaptive switching surface which makes the system to operate along a line in close proximity of the MPP loci. Obviously, MPPT would be satisfied if *S(V, i)* can be preserved in zero value, as shown in Fig. 4.

The controller produces the magnitude of the reference current i_{ref} as given by:

$$i^* = (K_P + K_I / s)\,(e_s + K\ \mathrm{sgn}(S)) \tag{16}$$

In (16), K_I and K_P represent the PI controller gains and K is the VSC gain. Using PV voltage and current, switching surface is calculated and then an error is defined as:

$$e_s = S^* - S \tag{17}$$

The intercept, *ref*, is set by a conventional MPPT control algorithm. So, P&O algorithm is selected because of its simplicity. A proper selection of slope introduced by constants *a* and *b*, can effectively reduce the MPPT's convergence time. So, we use least square estimate (LSE) method to the set of maximum power points correspond to different irradiation levels as an appropriate choice of slope. During transients, $e_s > K\ \mathrm{sgn}(S)$, and the Linear property is dominant. In the steady-state, error is very small and the

switching characteristic plays an important role. Also the *K* gain determines the ripple value. Adequate balance between

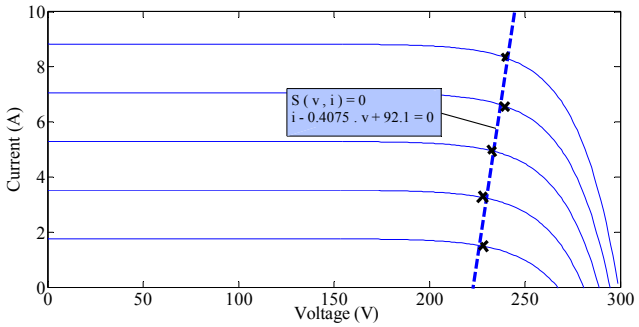

Fig.4 proposed switching surface [8]

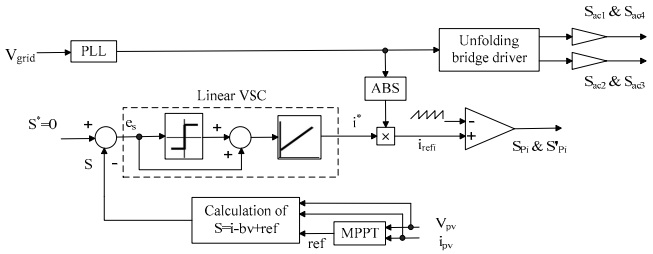

Fig.5 Block diagram of the proposed control system

linear and switching characteristic is easily obtained by proper gain selection. PI gains are chosen so that the linear control provides the desired dynamic response, while the VSC gain determines the robustness in steady-state operation. Phase locked loop (PLL) is used to detect the phase angle, amplitude and frequency of the grid voltage accurately and quickly to synchronize the reference (primary) current with the grid voltage and control the H-bridge inverter for unfolding purpose. The reference current is compared with a sawtooth waveform to produce switching signals for the main switches (S_{Pi} & S'_{Pi}). So, we have a fixed frequency to draw maximum power from PVG.

IV. PERFORMANCE EVALUATION

To evaluate the effectiveness of the suggested inverter and MPPT control system, several tests have been conducted on PSIM 9.0 software integrated with MATLAB software. The main parameters of the simulated system are listed in Table II. The appropriate switching surface is selected by applying LSE to the MPP loci. The resulting slope (normalized by *a*) is a = 1, b = 0.4075 and ref = 92.1. Waveforms of the simulated system during the grid period are plotted in Fig. 6. Reference current iref1 in (13) is followed by current waveform isp1 depicted in Fig. 6(a). Voltage waveform Vsp1 is plotted in Fig. 6(b). As it is depicted, the switch voltage is clamped to the dc input voltage V_{PV}. Waveforms of the simulated system during the switching period are depicted in Fig. 7. Switching signals GSP1, GSP2 and GSP3 are given to the switches SP1, SP2 and SP3 respectively shifted at 120° to have lower ripple [7] which has been plotted in Fig. 7(a). Current waveforms iSP1, iSP2 and iSP3 and output rectifier diode currents iD"1, iD"2 and iD"3 are shown in Fig. 7(b) and 7(c) respectively. Clamping diode currents iD1, iD2 and iD3 are displayed in Fig. 7(d). Fig. 7(e) illustrates voltage waveform VSP1. According to the simulation results, the predicted waveforms of Fig. 3 are confirmed with the simulation waveforms. Fig.8 shows the simulation results of MPPT control. The irradiation changes from 1000 W/m^2 to 800 W/m^2. The sliding-mode MPPT, is compared with an ordinary "PWM based MPPT". The sliding mode MPPT is seen to converge within 7 ms with the MPPT step size of ref = 0.4, whereas the PWM based MPPT converges within 0.5 s. Fig. 9 shows switching surface values. Based on these results, it can be concluded that the proposed MPPT control has a fast and robust response in comparison with PWM based MPPT. Fig.10 shows the simulated waveforms of the grid voltage and current. The grid current has 2% THD and the power factor of 99.96. The waveforms demonstrate the success of the proposed control system and the proposed PV inverter system in achieving the high quality energy transfer into the grid.

TABLE II. SIMULATION PARAMETERS OF THE PROPOSED SYSTEM

Parameter	Value	Unit
Switching frequency f_{sw}	20	kHz
Grid frequency f_{grid}	50	Hz
Transformers turn ratio (Np/Ns)	0.33	
Nominal power	2000	W
Magnetizing inductance L_m	78	µH
Leakage inductance L_{lk}	0.78	µH
Input capacitance C_{in}	5.3	mF
Filter inductance Lf	0.3	mH
Filter capacitance C_f	0.35	µF

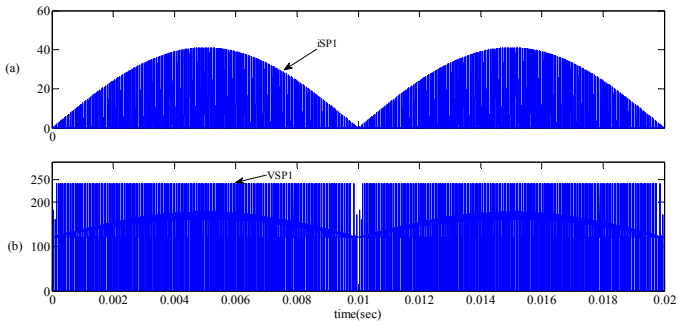

Fig.6. Performance of the suggested system under full load condition during grid period

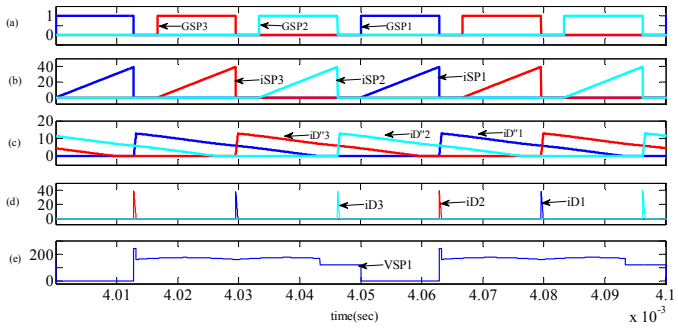

Fig.7. Performance of the suggested system under full load condition during switching period

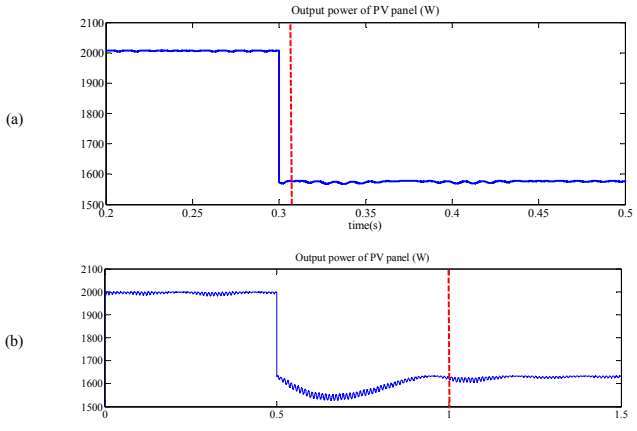

Fig.8: Output power of PV Panel, (a) proposed variable structure control, (b) PWM based MPPT

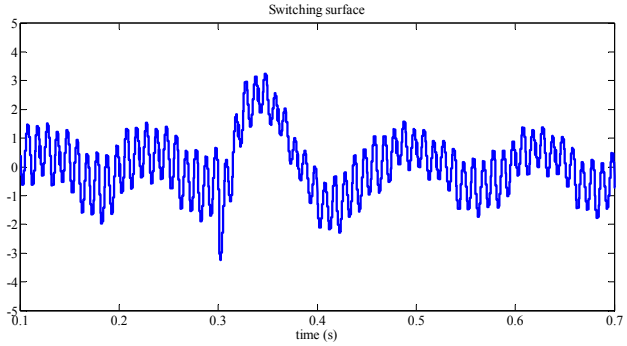

Fig.9: Switching surface values

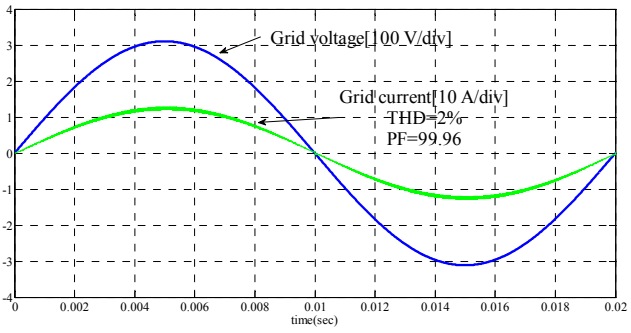

Fig .10 simulated waveform of the grid voltage and current

V. CONCLUSION

A string-type PV inverter for small electric power system applications rated at 2 kW is designed and simulated based on the two switch flyback converter topology. This inverter system consists of three interleaved two switch flyback cells each rated at 700 W limiting the high-voltage transients of the switches to the dc input voltage. Also a linear variable structure MPPT control was presented which can fix the switching frequency, while the fast response and robustness merits of the sliding mode controller. The simulation results demonstrate the successful operation of the inverter and compliance to the specifications. The THD of the grid current is measured as 2% and the power factor is 0.996, which are verifying the high power quality interface to the grid. Therefore, it is shown that interleaved two switch flyback topology is an appropriate topology at high power as a string-type PV inverter.

REFERENCES

[1] S. B. Kjaer, J. K. Pedersen, and F. Blaabjerg, “A review of single-phase grid-connected inverters for photovoltaic modules,”IEEE Trans. Ind.Appl., vol. 41, no. 5, pp. 1292–1306, Sep. 2005

[2] Young-Ho Kim, Young-Hyok Ji, Jun-Gu Kim, Yong-Chae Jung, and Chung-Yuen Won , “A New Control Strategy for Improving Weighted Efficiency in Photovoltaic AC Module-Type Interleaved Flyback Inverters, IIEEE Trans Power Electron, VOL. 28, NO. 6, JUNE 2013

[3] Murthy-Bellur and Kazimierczuk, M.K. “Zero-current-transition TWO-Switch flyback pulse-width modulated DC-DC converter,” Power Electronics, IET, P. 288–295 March 2011.

[4] Dakshina Murthy Bellur, “Hard-switching and soft- switching two-switch flyback PWM DC-DC converters and winding loss due to harmonics in high-frequency transformers,” Ph.D. dissertation, WRIGHT STATE university, 2010.

[5] Mohammadi, S.; Zarchi, H.A.; Amiri, M., "Interleaved two-switch flyback microinverter for grid-tied photovoltaic applications," *Power Electronics, Drives Systems & Technologies Conference (PEDSTC), 2015 6th*, vol., no., pp.59, 64, 3-4 Feb. 2015

[6] Tamyurek, B.; Kirimer, B., "An Interleaved High-Power Flyback Inverter for Photovoltaic Applications," *Power Electronics, IEEE Transactions on*, vol.30, no.6, pp.3228, 324, June 2015

[7] Z. Zhang, X.-F. He, and Y.-F. Liu, “An optimal control method for photovoltaic grid-tied-interleaved flyback microinverters to achieve high efficiency in wide load range,”IEEE Trans. Ind. Appl., vol. 28, no. 11, pp.5074–5087, Nov. 2013.

[8] Levron, Y.; Shmilovitz, D., "Maximum Power Point Tracking Employing Sliding Mode Control," in *Circuits and Systems I: Regular Papers, IEEE Transactions on*, vol.60, no.3, pp.724-732, March 2013

[9] Ravari, F.K.; Zarchi, H.A., "A fast and robust maximum power point tracker for photovoltaic systems using variable structure control approach," in *Electrical Engineering (ICEE), 2015 23rd Iranian Conference on* , vol., no., pp.1647-1652, 10-14 May 2015

[10] Abraham I. Pressman, Keith Billings and Taylor Morey, Switching Power Supply Design, 3rd Ed. McGraw-Hill, 2009, pp.157-160.

[11] Kyritsis, A.Ch.; Tatakis, E.C.; Papanikolaou, N.P., "Optimum Design of the Current-Source Flyback Inverter for Decentralized Grid-Connected Photovoltaic Systems," *Energy Conversion, IEEE Transactions on* , vol.23, no.1, pp.281,293, March 2008